IEEE ISIE 2006, July 9-12, 2006, Montréal, Québec, Canada

An Alternate Priority Planning Algorithm for Dual-Arm Systems

Jen-Hui Chuang[+], Chien-Chou Lin[++] and Tsun-Hou Chou[+]

+Depart. of Computer Science,
National Chiao Tung University
1001 Ta Hsueh Road, Hsinchu, Taiwan 300, R.O.C.
Tel:+(886)3-573-1935, Email:jchuang@cs.nctu.edu.tw

++Depart. of Computer Science and Information Engineering,
Shu-Te University
No. 59, Hunshan Rd., Yenchau, Kaohsiung, Taiwan 824, R.O.C.
Tel:+(886)7-6158-000, Email: jacoblin@mail.stu.edu.tw

Abstract **–An alternate priority path planning algorithm for dual-manipulator systems is proposed in this paper. A master-slave architecture is used to deal with the coordination of two manipulators by alternately identifying configurations of the two manipulators. The proposed method utilizes a generalized potential field to evaluate repulsion between manipulators and obstacles in a workspace, so collision avoidance of the planned path can be guaranteed. The simulation results show that proposed algorithm is efficient, even in a narrow passage.**

Index Terms – dual-manipulator system, potential model, path planning, collision avoidance, 3-D workspace

I. INTRODUCTION

Path planning of robot systems has been studied widely in recent years [1-18]. The major part of the researches are proposed for a single-robot system. While only one robot in a workspace limits the classes of tasks that can be performed, a multi-robot system can expand the application area of robots. For example, a dual-manipulator system is more efficient than a single-manipulator system since the tasks can be processed in parallel. Nevertheless, the planning of a dual-manipulator system is more difficult than a single-manipulator system. In general, the algorithms of multi-robot systems [5-7, 12, 16, 17] can be divided into two basic approaches: centralized planning [5, 6, 13, 16, 17] and decoupled planning [7, 18]. The centralized approaches consider the planning of all robots together in a composite space. Some of the centralized approaches are extended from the algorithms for a single-robot system directly. For example, the randomized potential-field method (RPP) plans the path of two disc robots in a six-dimensional space, named composite C-space, which is the Cartesian product of the individual C-space of two robots. The planner is similar as in a single-robot system, but the dimension of its search space is doubled. As a result, the computing complexity increases dramatically.

Unlike the centralized approaches, the decoupled approaches [7, 18] first plan a path for each robot and then consider the interactions among these paths. The decoupled approaches are more efficient than centralized approaches, but they may not plan a path successfully. In other word, most of these approaches are not complete. For example, the fixed priority approach plans the path of each robot individually according its priority. It is obvious the algorithm will fail for some special cases. However, the performance of the fixed priority approach is better than centralized ones in most cases.

In this paper, we propose a novel decoupled path planning approach, named alternate priority planning algorithm, for an dual-manipulator system. The proposed method uses a master-slave architecture to deal with the coordination of two manipulators, by alternately identifying the two manipulators as a master robot and a slave robot, respectively. Unlike the fixed priority approach, master and slave robots plan their paths alternatively. Firstly, the master manipulator plans a path to an intermediate goal by considering the slave manipulator as a static obstacle. Then, the slave manipulator plans a path to another intermediate goal by considering the master manipulator as a static obstacle.

Since different robots are considered as obstacles at different time, the algorithm should re-compute the environment parameters all the time. Similar to the algorithm in [19] which uses a potential model to compute every configuration of a single-manipulator, the proposed algorithm also uses the potential model [20] to adjust robots for safe configurations.

The remainder of this paper is organized as follows. In Section II, we propose the alternate priority planning algorithm and the implementation details. A simulation considering a realistic situation is presented in Section III to show the effectiveness of the proposed algorithm. Section IV concludes this paper and outlines some possible directions for future researches. The adopted potential model [20] is reviewed in Appendix.

II. AN ALTERNATE PRIORITY PLANNING ALGORITHM

In this section, the alternate priority planning algorithm for dual-arm robots is described. While some centralized based approaches often require expensive computation time to explore a large-dimensional composite space, the decoupled planning scheme is adopted in this paper to reduce the search space. Like a single-robot system, the approach models the workspace wherein obstacles surfaces and robot links are assumed to be charged and computes, similar to that done in electrostatics, repulsive forces and torque between the manipulator and obstacles. Using these forces and torque formed by the potential model, manipulators adjust their configurations toward safe configurations, the minimum potential configurations.

A. Scenario

The scenario of this work involves two manipulators trying to position their end-effectors to their goals while avoiding obstacles (including another manipulator), as shown in Fig. 1. The two manipulators are specified as the master manipulator (Master) and the slave manipulator (Slave), respectively.

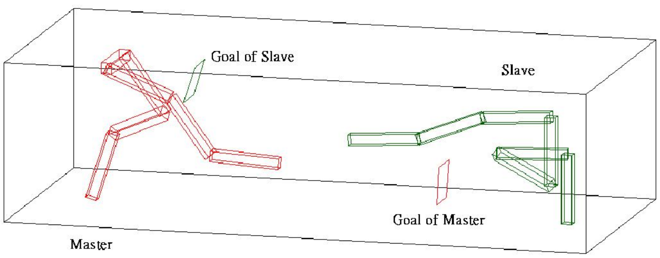

Fig. 1 A dual-manipulator system has two 7-link manipulators, Master and Slave, their goals.

B. Alternate Priority Planning Algorithm

The alternate priority algorithm has two stages. The first stage is Master stage. Master adjusts its configuration by using the repulsion between Master and obstacles, including Slave. Once the adjustment of Master has done, the slave begins to move toward its intermediate goal and adjusts its configuration by using the repulsion between Slave and obstacles, including Master. These two stages are processed iteratively until both manipulators reach their goals. The flowchart of the proposed algorithm is shown in Fig. 2. In Fig. 2, Master first moves its end-effector toward the goal, a goal plane, for an initial distance, δ. In general, the number of configurations and the computation time depends on δ. The smaller size the δ is set initially, the more configurations the planned path has. On the other hand, if δ is too large, the computation time also increases because collisions may occur frequently. The initial distance of this paper is predetermined as 10% of the workspace size.

The moving direction is along the direction of the attractive force experienced by end-effector due to the goal plane. In the far field, the attraction has a near spherical symmetry and is attracted toward the goal as if goal is a point attractor. In the near field, attraction will lead the end-effector toward the goal approximately in the normal direction of goal plane. The force magnitude is not used here. If the movement of Master is done, the movement of Slave is performed. For the dual-manipulator systems, the movements of Master and Slave are performed alternately.

The adjustment of the single robot mentioned above can be divided into two stages: (i) translating links toward the goal and (ii) searching for the minimum potential configuration of the manipulator. In (i), translating of all manipulator links except for the two base links does not perform configuration improvement to reduce the repulsive potential. When the pure translation of manipulator has finished, the potential minimization in (ii) is performed under some constraints of the distal link.

In (ii), links of the manipulator are adjusted from the distal link to the base link using the repulsion experienced by the manipulator. The associated constrained optimization problem is divided into two iterative univariant optimization procedures as followings: (ii-a) The distal link is fixed in its orientation and slides on the intermediate goal plane, which is formed by the norm of attraction and the point of the end-effector, to search for the minimal potential configuration and other distal links are sequentially adjusted in orientation, starting from the link connected to the distal link. (ii-b) The distal link is adjusted in orientation while fixed in position, which is determined by (ii-a), and the procedure for adjusting the rest links is similar to that in (ii-a).

Such a local path planning algorithm of a robot ends as the end-effector reaches the minimum potential of the intermediate goal plane or exits abnormally for an infeasible problem. Detailed implementation of the algorithm is presented next.

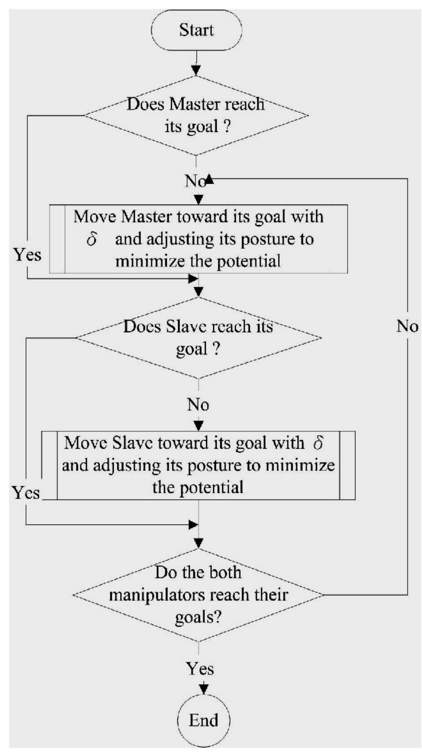

Fig. 2 The flowchart of the proposed algorithm, an alternate priority planning algorithm.

C. Adjusting A Manipulator Configuration By Potential

The local path planning algorithm of a manipulator is described as below:

(1) Translate all links, except the two base links, of the manipulator R_i with distance δ_i to move its end-effector along the direction of attraction of the goal plane. Find the smallest $n \neq 0$ such that

$\delta \leftarrow \delta / 2^n$ corresponds to a feasible and collision-free translation. If the manipulator can't move anymore, go to Step (6); otherwise, construct a intermediate goal plane with the norm of the attraction and the point of the end-effector.

(2) Translate the distal link by sliding the end-effector on the intermediate goal plane to minimize the potential.

(3) Adjust joint angle of the manipulator for the minimum potential configuration with the end-effector fixed in position.

(4) Go to Step (2) if the translation in Step (2) or the joint angle adjustment in Step (3) is not negligible.

(5) Stop here and go to Step (1) with another manipulator.

(6) Exit and report that goal is unreachable.

D. *Generalized Potential Model*

In 3-D environment, the free space is modeled by considering the potential due to uniform source distributions on surfaces of robots and obstacles. The repulsion experienced by an object of finite size due to the potential gradient is considered. It is shown that the repulsion between polygonal object and obstacles, in forms of force and torque, can be derived in closed form. In [20], a generalized potential model which assures collision avoidance between a point and polyhedral surfaces in the 3D space was proposed. The potential function is inversely proportional to the distance between two point charges to the power of an integer (m).

$$\int_S \left(dS / R^m\right) \quad , \quad m \geq 2 \qquad (1)$$

where $R = |r' - r|$, $r' \in S$, and integer m is the order of the potential function. In particular, it is shown that the repulsive force exerted on a point charge due to a 3-D polygon can be obtained analytically by evaluating the gradient of the potential function for (m=3)

$$\int_S \frac{dS}{R^3} \triangleq \Phi(x,y,z) = \sum_i \left[\phi(x_2^i, y_2^i, z) - \phi(x_1^i, y_1^i, z)\right] + \frac{\alpha}{z} \qquad (2)$$

with (see Appendix)

$$\phi(x,y,z) = \frac{1}{z}\tan^{-1}\frac{xz}{y\sqrt{x^2+y^2+z^2}} \quad , \qquad (3)$$

where the x^i-y^i-z coordinate system is determined by the right-hand rule for each edge i of the polygon such that z is measured along the normal direction and x^i is measure along edge i of the polygon, respectively, and α is a constant. Hence, the robots are represented by charged points and obstacles represented by charged polygons. By using (2), the repulsive force exerted on the robot due to obstacles can be denoted as

$$f = \sum_i^m \Big(\sum_j^n f_{i_x}^j, \sum_j^n f_{i_y}^j, \sum_j^n f_{i_z}^j\Big) = \sum_i^m \Big(\sum_j^n \frac{\partial \Phi_i^j}{\partial x}, \sum_j^n \frac{\partial \Phi_i^j}{\partial y}, \sum_j^n \frac{\partial \Phi_i^j}{\partial z}\Big) \qquad (4)$$

where m is the number of charged points, n is the number of obstacle polygons and

$$\frac{\partial \Phi_3}{\partial x} = \frac{y}{(x^2+y^2)\sqrt{x^2+y^2+z^2}} , \qquad (5)$$

$$\frac{\partial \Phi_3}{\partial y} = \frac{-x(x^2+2y^2+z^2)}{(x^2+y^2)(y^2+z^2)\sqrt{x^2+y^2+z^2}} , \qquad (6)$$

$$\frac{\partial \Phi_3}{\partial z} = -\frac{\tan^{-1}\frac{xz}{y\sqrt{x^2+y^2+z^2}}}{z^2} + \frac{xy(x^2+y^2)}{z(x^2+y^2)(y^2+z^2)\sqrt{x^2+y^2+z^2}} \qquad (7)$$

III. Simulation Results

In this section, we show the effectiveness of the proposed algorithm for path planning of dual-arm systems in a static environment. The simulations are implemented in C++ on a Pentium IV 2.4G PC with Windows XP system.

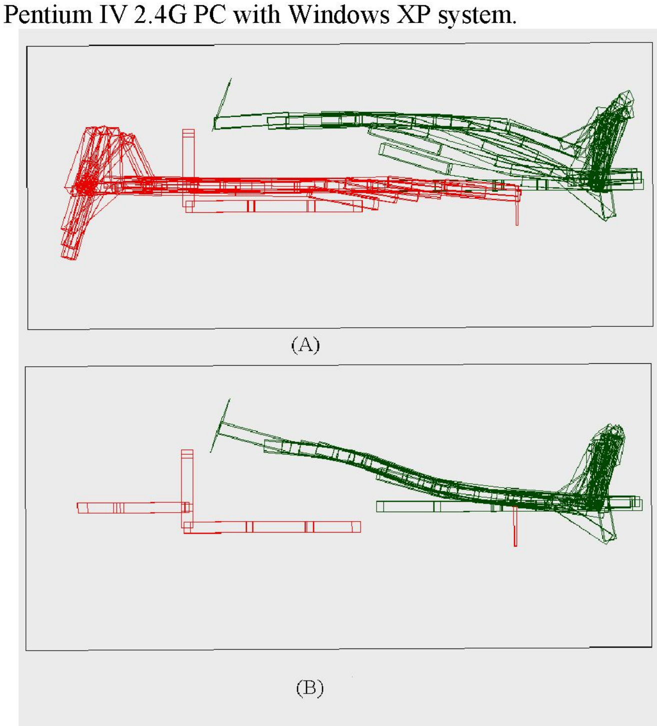

Fig. 3 (a) The planned paths of the example shown in Fig. 1. (b) The planned path of Slave when Master is fixed.

Fig. 3(a) shows the planned trajectories of a dual-arm system. The initial configuration of this example is shown in Fig. 1. The proposed algorithm plans an eight-configuration path for Master and a nine-configuration path for Slave. The total computation time is 2.281 seconds (0.188s for Master and 2.093s for Slave). Fig. 3(b) shows another planned trajectory of Slave when Master is fixed in its initial configuration. Comparing the two trajectories in Figs. 3(a) and (b), it is obviously that Slave detours to avoid Master in Fig. 3(a).

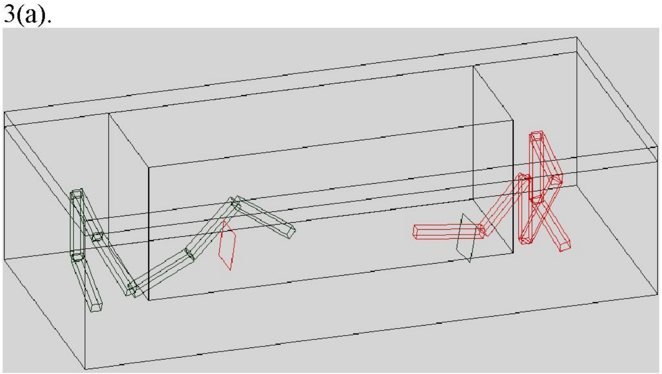

(a)

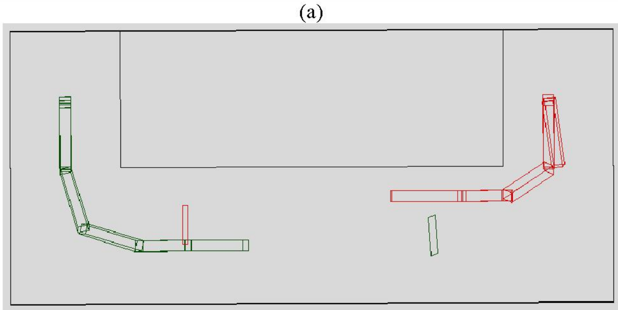

(b)

Fig. 4 An example of the dual-manipulator system within a narrow passage. (a) The initial configurations of two manipulators. (b) The top view of the initial configurations.

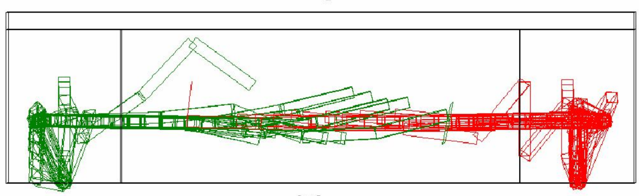

(a)

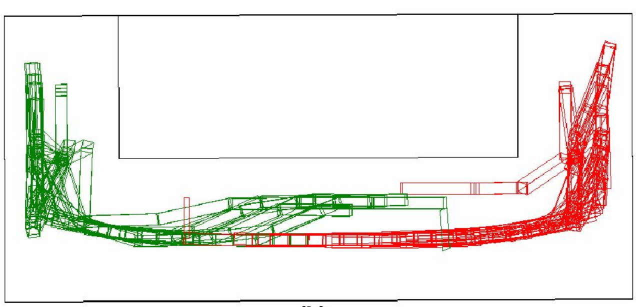

(b)

Fig. 5 The planned paths of the example shown in Fig. 4. (a) The side view. (b) The top view.

Another example is shown in Fig. 4. Figs. 4(a) and (b) show the initial configurations of manipulators within a narrow passage. Both Master (right) and Slave (left) are seven links connecting with 3D joints. The planned path of the manipulators is shown in Figs. 5(a) and (b) for the side view and the top view of the planned trajectories, respectively. The both paths of two robots are eleven configurations. The total computation time is 4 seconds (0.797s for Master and 3.203s for Slave). It is easy to see that the proposed algorithm also works well in a narrow passage in this simulation.

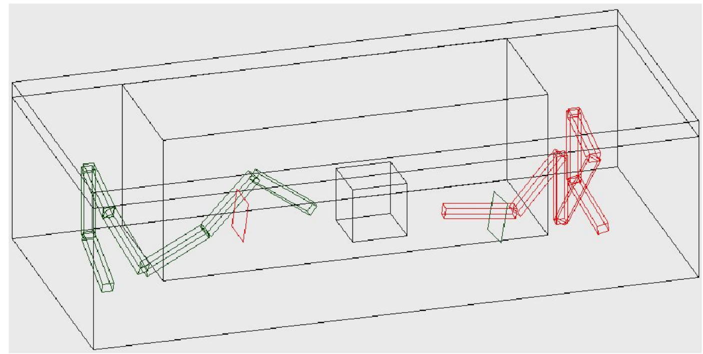

(a)

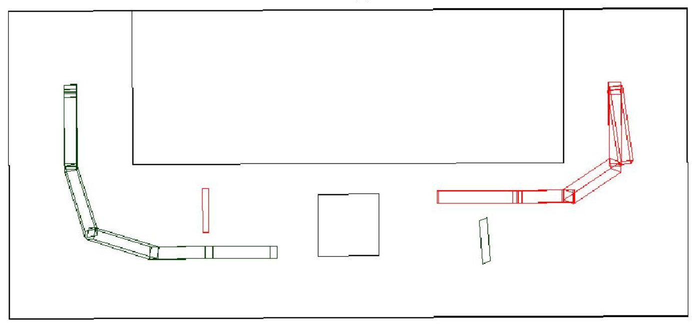

(b)

Fig. 6 An example of the dual-arm system within a narrow passage. (a) The initial configurations of two manipulators. (b) The top view of the initial configurations.

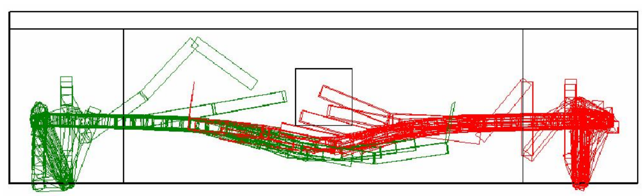

(a)

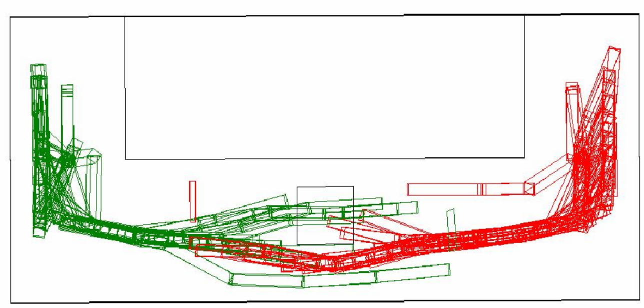

(b)

Fig. 7 The planned paths of the example shown in Fig. 6. (a) The side view. (b) The top view.

Figs. 6(a) and (b) show the initial configurations of manipulators. This example is similar to the example in Fig. 4 but with an additional obstacle in the narrow passage. This example demonstrates the flexibility of the proposed algorithm. Figs. 7(a) and (b) show the planned path of the manipulators from the top view and side view, respectively. The trajectory of Master is locating at the central space of the passage. In this example, both of Master's and Slave's trajectories have 14 configurations. As the free space is more congested, the planning is more time-consuming with total computation time equal to 5.906 seconds (1.703s for Master and 4.203s for Slave). As shown in Fig. 7(a), the planned paths are located in the lower place because of the extra obstacle. It is easy to see that the trajectory of Slave dangles to one side significantly in Fig. 7(b).

IV. Conclusions

In this paper, an alternate priority algorithm for dual-arm systems is proposed to solve path planning problems in various 3-D workspaces wherein a dynamic scheme is adopted to assign priorities of the two robots.

Firstly, the high-priority robot (Master) plans a local path to its intermediate goal using the repulsion from obstacles and Slave. Then, Slave plans its local path using the repulsion from obstacles and Master. A generalized potential model is adopted to ensure collision free. The artificial potential field models the workspace such that obstacles surfaces are assumed to be charged uniformly while each manipulator is represented as a set of charged sampling points. The repulsive force and torque between manipulator and obstacles thus modeled are used for adjusting the manipulator to a safe position during path planning.

It is easy to see from the simulation results that planned paths are always spatially smooth. It also gives a demonstration that the algorithm works well in a narrow passage. Furthermore, the proposed algorithm is quite efficient compared with similar algorithms. For a dual-arm system with 7-link robots, the planning time is no more than a few seconds for some reasonable environments.

V. Appendix

In this section, the generalized potential model [20] is reviewed. Consider a planar surface S in the 3-D space, the direction of its boundary, ΔS, is determined with respect to its surface normal, $\hat{n}$, by the right-hand rule, $\hat{u}\times\hat{l}=\hat{n}$, where $\hat{u}$ and $\hat{l}$ are along the (outward) normal and tangential directions of ΔS, respectively. For the generalized potential function, the potential value at **r** is defined as (1). The Newtonian potential (m=1) is harmonic in the 3-D space and can not prevent the robot from colliding the obstacles, and thus can not be used for collision avoidance. The basic procedure to evaluate the potential at **r** can be summarized as follows:

i. Write the integrand of the potential integral over S as surface divergence of some vector function.
ii. Transform the integral into the one over ΔS based on the surface divergence theorem.
iii. Evaluate the integral as the sum of line integrals over edges of ΔS.

Without the loss of generality, it is assumed that

$$d \overset{\Delta}{=} \hat{n}\cdot(r-r')>0 \qquad (8)$$

which is equal to the distance from **r** to Q. For (i), we have

$$\frac{1}{R^m}=\nabla_S\cdot(f_m(R)\mathbf{P}) \qquad (9)$$

where **P** is the position vector of **r'** with respect to the projection of **r** on Q, $\mathbf{r}_Q$, and

$$f_m(R)=\frac{1}{P^2}\int R^{m-1}dR = \begin{cases} \dfrac{\log R}{R^2-d^2}, & m=2 \\ \dfrac{-1}{(m-2)R^{m-2}(R^2-d^2)}, & m\neq 2 \end{cases} \qquad (10)$$

Note that if $\mathbf{r}_Q$ is inside S, $f_m(R)$ will becomes singular for some $\mathbf{r}''=\mathbf{r}_Q$, (and $R=d$). Let $S\varepsilon$ denote the intersection of S and a small circular region on Q of radius ε and centered at $\mathbf{r}_Q$, the potential due to S can be evaluated as

$$\begin{aligned}\int_S \frac{dS}{R^m} &= \lim_{\varepsilon\to 0}\left[\int_{S-S_\varepsilon}\nabla_S\cdot(f_m(R)\mathbf{P})dS+\int_{S_\varepsilon}\frac{dS}{R^m}\right] \\ &= \int_{\Delta S} f_m(l)\mathbf{P}\cdot\hat{\mathbf{u}}dl+\lim_{\varepsilon\to 0}\left[-\int_0^{\varepsilon}\varepsilon^2 f_m(\sqrt{\varepsilon^2+d^2})d\theta+\int_0^{\alpha}\int_0^{\varepsilon}\frac{pdpd\theta}{(p^2+d^2)^{\frac{m}{2}}}\right] \\ &= \sum_i \mathbf{P}_i^0\cdot\hat{\mathbf{u}}_i\int_{C_i} f_{m,i}(l_i)dl+g_m(\alpha), \end{aligned} \qquad (11)$$

where

$$f_{m,i}(l_i)=f_m(R=\sqrt{l_i^2+d^2+(P_i^0)^2}), \qquad (12)$$

$$g_m(\alpha)=\begin{cases}\alpha\log d, & m=2 \\ \dfrac{\alpha}{(m-2)d^{m-2}}, & m\neq 2\end{cases}$$

P_i^0 is the distance between $\mathbf{r}_Q$ and C_i, l_i is measured from the projection of **r** on C_i along the direction of $\hat{l}_i$, and α is the angular extent of the circumference of $S\varepsilon$ lying inside S as $\varepsilon\to 0$. The $m=3$ is considered and we have

$$\int_C f_3(l)dl=\frac{1}{P^0 d}\left[\tan^{-1}\frac{l^- d}{P^0 R^-}-\tan^{-1}\frac{l^+ d}{P^0 R^+}\right] \qquad (13)$$

with R^- and R^+ equal to the distances from **r** to the two end points of C_i, respectively. Thus, the repulsive force exerted on a point charge due to S can be found analytically by evaluating the gradient of the following function

$$\Phi_3(x, y, z) = \frac{1}{z}\tan^{-1}\frac{xz}{y\sqrt{x^2+y^2+z^2}} \quad (14)$$

at some (x, y, z)'s.

ACKNOWLEDGEMENT

This work is supported by National Science Council of Taiwan under grant no. NSC 94-2213-E-366 -011.

REFERENCES

[1] R. R. Murphy, C. Lisetti, R. Tardif, L. Irish, and A. Gage, "Emotion-based control of cooperating heterogeneous mobile robots," *IEEE Trans. Robot. & Auto.*, pp. 744–757, 2002.

[2] D. Jung and A. Zelinsky, "Grounded symbolic communication between heterogeneous cooperating robots," *Auton. Robots*, vol. 8, no. 3, pp.269–292, 2000.

[3] C. Chang, M.-J. Chung, and B.-H. Lee, "Collision Avoidance of Two General Robot Manipulators by Minimum Delay Time," *IEEE Trans. on Sys., Man, and Cyber., Vol. 24, NO. 3, pp. 517-522, 1994.*

[4] K.-S. Hwang, M.-Y. Ju and Y.-J. Chen, "Speed Alteration Strategy for Multijoint Robots in Co-Working Environment," *IEEE Trans. on Industrial Electronics, vol. 50, no. 2, pp. 385- 393, 2003.*

[5] J. Barraquand and J.-C. Latombe, "Robot Motion Planning: A Distributed Representation Approach," *Int. Jour. of Rob. Res., 10(6):628-649, 1991.*

[6] M. Erdmann and T. Lozano-Perez, "On Multiple Moving Objects," *Algorithmica, Vol. 2, pp. 477-521, 1987*

[7] K. Gupta and S.-W. Zucker, "Toward Efficient Trajectory Planning: Path Velocity Decomposition," *Int. Jour. of Rob. Res., Vol. 5, pp. 72-89, 1986.*

[8] Y. Koga and J.-C. Latombe, "On Multi-Arm Manipulation Planning," *Proc. of the IEEE Int. Conf. on Rob. & Auto. (ICRA), pp. 945-952, 1994.*

[9] J.-C. Latombe, "Robot Motion Planning," *Kluwer Academic Publishers, Boston, MA, 1991.*

[10] F. Chantemargue and B. Hirsbrunner, "A collective robotics application based on emergence and self-organization," in *Proc. 5th Int. Conf. Young Computer Scientists*, 1999, pp. 1–8.

[11] S. Akella and J.-F. Pen, "Time-Scaled Coordination of Multiple Manipulators," *Proc. of the IEEE Int. Conf. on Rob. & Auto. (ICRA), pp. 3337- 3344, 2004.*

[12] K. Passino, "Biomimicry of bacterial foraging for distributed optimization and control," *IEEE Contr. Syst. Mag.*, vol. 22, pp. 52–67, June 2002.

[13] T.-Y. Li and J.-C. Latombe, "On-Line Manipulation Planning for Two Robot Arms in a Dynamic Environment," *Int. Jour. of Rob. Res., 16(2):144-167, 1997.*

[14] S. Brueckner and V. D. Parunak, "Multiple pheromones for improved guidance," in *Proc. 2nd Symp. Advanced Enterprise Control*, Minneapolis, MN, July 2000.

[15] T. Balch, "The impact of diversity on performance in multi-robot foraging," in *Proc. 3rd Int. Conf. Auton. Agents*, 1999, pp. 92–99.

[16] M. Sharir and S. Sifrony, "Coordinated Motion Planning for Two Independent Robots," *Symposium on Computational Geometry, 1988, pp. 319-328*

[17] P. Tournassoud, "A strategy for obstacle avoidance and its application to multi-robot systems," *Proc. of the IEEE Int. Conf. on Rob. & Auto. (ICRA), pp. 1224--1229, 1986.*

[18] S. J. Buckley, "Fast Motion Planning for Multiple Moving Robots," *Proc. of the IEEE Int. Conf. on Rob. & Auto. (ICRA), pp. 322-326, 1989.*

[19] C.-C. Lin, J.-H. Chuang, "Potential-based path planning for robot manipulators in 3-D workspace," *IEEE Int. Conf. on Rob. & Auto. (ICRA), pp. 3353-3358, 2003.*

[20] J-H. Chuang, "Potential-based modeling of three-dimensional workspace of the obstacle avoidance," *IEEE Trans. on Rob. & Auto.*, vol. 14, no. 5, pp. 778-785, 1998.